GIG Research Institute

JOURNAL OF SUSTAINABLE MINING

Volume 21 | Issue 2 Article 8

2022

# Investigating the causes of stope instability at Golden Valley Mine

Author(s) ORCID Identifier:
Ashley Ruvimbo Sabao 0000-0002-7161-1402
Prosper Munemo 0000-0001-5126-5322
Peter Kolapo 0000-0002-8840-1284

Follow this and additional works at: https://jsm.gig.eu/journal-of-sustainable-mining

Part of the Explosives Engineering Commons, Oil, Gas, and Energy Commons, and the Sustainability Commons

## Recommended Citation

Sabao, Ashley Ruvimbo; Munemo, Prosper; and Kolapo, Peter (2022) "Investigating the causes of stope instability at Golden Valley Mine," *Journal of Sustainable Mining*: Vol. 21 : Iss. 2 , Article 8.
Available at: https://doi.org/10.46873/2300-3960.1354

This Research Article is brought to you for free and open access by Journal of Sustainable Mining. It has been accepted for inclusion in Journal of Sustainable Mining by an authorized editor of Journal of Sustainable Mining.

# Investigating the causes of stope instability at Golden Valley Mine


## Abstract

The study is based on mining operations that are concentrated in a ground exposed to flooding with varying stope dimensions. Stope stability was assessed in the four stopes, which resembled the mine's different ground conditions using the stability graph complemented by the equivalent linear over break slough (ELOS) stability approach. The stability graph showed that the stopes in rock masses exposed to flooding fell in the potentially unstable and caving zones whereas the ones that were not affected by flooding fell in the stable zones. The ELOS approach showed that mining the previously flooded rock masses resulted in high over-breaks in the stopes despite them having smaller hydraulic radii. Therefore, it was deduced that although stope extension plays a part in the over-breaks experienced in different stopes, it is not the main cause of the overall stope instability. The results confirm the supposition that over-break is largely controlled by pore pressure than it is by blast induced stresses. Continuous implementation of the old support systems was no longer compatible with the state of the ground conditions. Hence, the mine should implement 6 × 8 m pillars, which have an acceptable factor of safety against failure.



## Keywords

stability, flooding, stope, safety factor



## Creative Commons License

This work is licensed under a Creative Commons Attribution-Noncommercial-No Derivative Works 4.0 License.



This research article is available in Journal of Sustainable Mining: https://jsm.gig.eu/journal-of-sustainable-mining/vol21/iss2/8

RESEARCH ARTICLE

# Investigating The Causes of Stope Instability at Golden Valley Mine

Ashley R. Sabao [a,b], Prosper Munemo [a,*], Peter Kolapo [c]

[a] Manicaland State University of Applied Sciences, Department of Mining and Mineral Processing Engineering, Mutare, Zimbabwe
[b] Central South University, School of Resources and Safety Engineering, Changsha, China
[c] University of Kentucky, Department of Mining Engineering, USA

**Abstract**

**The study is based on mining operations that are concentrated in a ground exposed to flooding with varying stope dimensions. Stope stability was assessed in the four stopes, which resembled the mine's different ground conditions using the stability graph complemented by the equivalent linear over break slough (ELOS) stability approach. The stability graph showed that the stopes in rock masses exposed to flooding fell in the potentially unstable and caving zones whereas the ones that were not affected by flooding fell in the stable zones. The ELOS approach showed that mining the previously flooded rock masses resulted in high over-breaks in the stopes despite them having smaller hydraulic radii. Therefore, it was deduced that although stope extension plays a part in the over-breaks experienced in different stopes, it is not the main cause of the overall stope instability. The results confirm the supposition that over-break is largely controlled by pore pressure than it is by blast induced stresses. Continuous implementation of the old support systems was no longer compatible with the state of the ground conditions. Hence, the mine should implement 6 × 8 m pillars, which have an acceptable factor of safety against failure.**

*Keywords:* stability, flooding, stope, safety factor

## 1. Introduction

Villaescusa [1] argued that "the success of any open stope mining largely depends on the stability of un-reinforced stope walls and crowns as well as the stability of any exposed fill masses." However, the complexity in the spatial distribution of rock-mass properties during site investigations results in the variability of the rock-mass's physical and mechanical properties, which often leads to poor design. Kolapo [2] mentioned that, "the understanding of correct mechanisms of behaviour of rocks is an important part to successful planning, design criteria and choice of selecting a suitable factor of safety for deep underground openings." Due to the limited availability of geo-mechanical data during pre-feasibility and feasibility stages, most geotechnical design analysis is performed based on assumption and also on the use of discrete values of rock mass properties [3]. In such a design, the result of such analysis can lead to an unstable stope that can cause accidents due to variation in the design parameters.

The need for this study was raised by Golden Valley Mine, which is experiencing flooding at most of its mining levels. Prior to its flooding, mining operations at Golden Valley mine had progressed to 33-level. However, from the time the mine reopened to date, most of these levels have remained flooded. In order to sustain the mine until the levels are completely dewatered, the mine resorted to concentrate mining activities on the pre-mined stopes. This method would cause a significant increase in stope dimensions which would curb the financial problems of mines. However, it did not consider the issues that affect the stability of the stopes. According to Swart [4], some of the issues that influence rock engineering designs are the rock mass properties and potential failure modes. Instead, the new panel lengths were solely dictated by the expected monthly production targets. This increase in stope dimensions was successfully

Received 4 November 2021; revised 12 April 2022; accepted 16 April 2022.
Available online 10 August 2022

* Corresponding author at:
E-mail addresses: prosper.munemo@staff.msuas.ac.zw, munemoprosper@gmail.com (P. Munemo).

https://doi.org/10.46873/2300-3960.1354
2300-3960/© Central Mining Institute, Katowice, Poland. This is an open-access article under the CC-BY 4.0 license (https://creativecommons.org/licenses/by/4.0/).

implemented in all top levels but caused numerous ground stability problems from 21-level.

The geological alterations brought about as a result of flooding have made the rock mass behavior in this area highly unpredictable. Rock mechanics problems are now being encountered, evidenced by both local and regional instabilities occurring in these levels. Notably, ground falls have been occurring due to blasting and failure of both the existing in-panel pillars and installed support. It was clearly observed that the production stopes were heavily fractured and scaled, making them highly unstable.

The combinations of geological alterations in the host rock, inherent rock properties, and induced stresses have created unfavorable geotechnical conditions resulting in instability of the rock mass surrounding production excavations. Sudden rock bursts, slabbing, collapse, and ground movement continue to pose a danger to ground stability. The mine has since recorded numerous injuries among workers as a result of the ground instability issues. It has become challenging to meet the monthly production targets as stopes are temporarily closed for support reinforcement; hence there is a need to reduce these "stop and fix" scenarios. The mine has also lost a significant amount of money in compensating and also footing the medical bills for all the injuries that occurred and will continue losing its valuable revenue while meeting the above-mentioned avoidable expenses. It will also remain with a tainted reputation and a demotivated workforce due to low levels of safety in working areas if the problem of ground instability is not addressed with the immediate attention it deserves.

In order to solve these above-mentioned problems at Golden Valley Mine, this paper investigates the causes of instability at the mine with the primary aim of improving the ground condition by providing an alternative compatible support system. The rock mass classification approach of the Q-system was used to assess various ground conditions and properly classify the rock in each stope. The stability chart was also used as an alternative method to evaluate the stability of all four stopes. This would provide appropriate information about the ground conditions and support that is required to stabilize the roof before the installation of support systems.

## 2. Description of Golden Valley Mine

Golden Valley Mine is located 20 km west of Kadoma town in Mashonaland West province of Zimbabwe, as shown in Fig. 1.

The shear zone hosting the Golden Valley Mine ore bodies is about 10–15 m wide with a strike of approx. 1700 m, striking 10° north and dipping 35° west. The host rocks are massive and pillowed basalts and andesites which have been intruded by quartz porphyry sheets. The gold bearing reef is cut by an east-west trending normal fault zone (pioneer fault), resulting in two discrete ore bodies, the south ore body dips at 27–30° and the north ore body dips at 33–37°. The northern ore body is characterized by reefs of smaller width and greater gold content, whilst the southern side has reefs of wider width

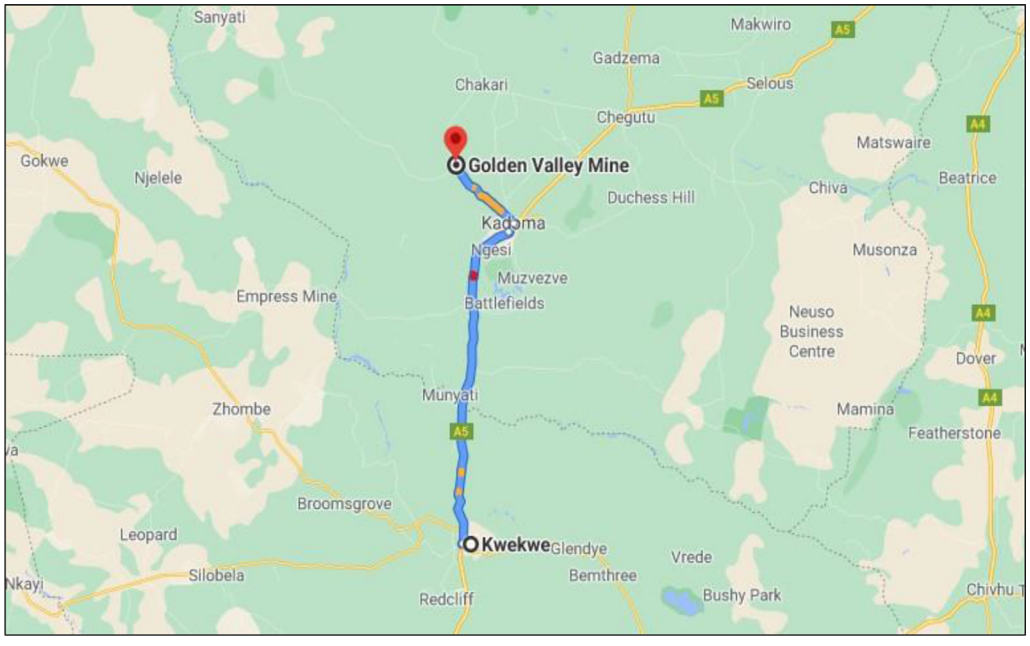


*Fig. 1. Geographic location of Golden Valley Mine, google maps [5].*

and lesser gold content. The Maida Vale fault, Golden Valley fault, and other small terminal faults also cut the reefs at various points.

The mine extracts ore deposits using sublevel open stoping which is an underground mining method used in competent ground conditions that require minimum or no support. The method involves the creation of large open areas known as 'stopes' and is used in large steep dipping ore bodies. An average stope height of 2.0 m usually is maintained, but it can be increased to 2.5 m in cases where the footwall will have a high grade. Support installations follow mine standards based on the joint strike directions and the brows created due to mining and the presence of fault intrusions. Pillars, usually with dimensions of 4 × 4 m, are left behind randomly to support the stopes. In cases where the stopes have advanced, the support system is improved by installing timber props in conjunction with mat packs.

## 3. Stope stability in open stope mines

A fundamental step in the design of any proposed underground excavation is evaluating of both the natural stability and mechanical modes of instability in the design of the support system in order to minimize their failure [6]. Instability in mining operations is mainly due to high stress to strength ratio conditions, structurally controlled mechanisms, or induced stresses and geological structures. Generally, the stability of excavations that are closer to the surface controlled by geological structures, whereas in deep excavations, stability is governed by natural in situ stresses. At medium depths in weak rocks and at considerable depths in solid rocks, natural stress which is usually altered by the mining excavation, can be a major problem. According to Kolapo [7], the uniaxial compressive strength (UCS) of the rock mass is the most important mechanical property of rocks used in geo-engineering to analyse the stability of underground structures.

### *3.1. Factors that cause rock mass failure*

Failure in rocks occurs when the imposed stresses overcome the rock strength. The strength of a rock can be described as the extent to which a rock specimen can tolerate the process of stress redistribution before it fails. Therefore, processes that tend to increase the stress redistributions in rocks increase failure chances. According to Brahimaj [8], some common factors and processes that promote rock failure are increased pore pressure, cracking, swelling, decomposition of clay rock fills, creep under sustained loads, leaching, and strain softening, weathering and cyclic loading.

As mentioned earlier, the case study mine has most of its stopes submerged in water; thus review of the effects of water on stope stability has been done in this paper. According to Brahimaj [8], the influence of water on the rock masses is a two-fold problem, that is, firstly, ground water generates pore water pressure, and secondly, rainwater infiltration generates water pressure along the geological discontinuities. Both effects are influenced by the rainfall patterns in the area as well as the hydrological properties of the rock mass under consideration. Brahimaj [8] mentioned that "water pressure acting within a discontinuity reduces the effective normal stress acting on the plane and this, in turn, reduces the shear strength of the discontinuity plane." Figure 2 illustrates how water typically affects the stability of rock masses, whereby water applies horizontal and vertical pressure along the discontinuity plane.

In addition to ground water, rainfall water also adds weight to the rock mass. Such water replaces the air in the pore space, thereby increasing the weight of the rock. This leads to an increase in the effective stress failing the underground openings [8].

### *3.2. Application of rock mass classification in open stope mining*

Stacey [9] mentioned that, "a rock mass is generally weaker and more deformable than its constituent rock material as the mass contains structural weakness planes such as joints and faults." The stability of excavations in jointed rock masses is influenced by the strength of rock material, frequency of jointing, joint strength, confining stress, and presence of water [9]. Therefore, rock classification systems can be used to account for the weakening effects in rock masses.

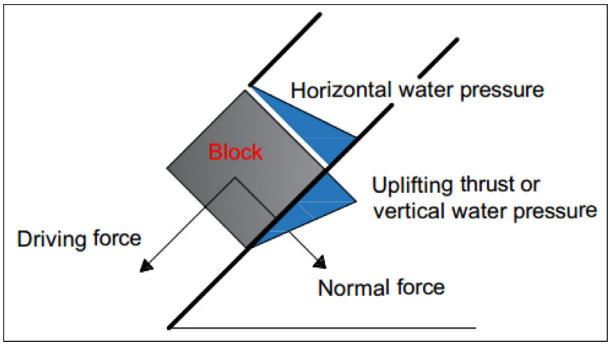


*Fig. 2. Effect of water on discontinuity planes [8].*

Lauffer [10] came up with a system that links the rock types to the stand-up time of any unsupported active span. The system explains how an increase in this span leads to a significant reduction in the time available for installing support (known as the stand-up time). In designing the support for hard rock excavations, it is prudent to assume that the stability of the rock mass surrounding the excavation is not time dependent [11]. Pacher [12] modified Lauffer's system such that the method now includes a number of techniques for safe tunneling in rock conditions where the stand-up time is limited before failure occurs.

The Norwegian Geotechnical Institute (NGI) also proposed an index ($Q$) to determine of the quality of rock mass. The index values are linked to different types of permanent support by means of a schematic support chart [13]. According to NGI [13], the calculated value can be used to determine the type and quantity of support that has been successfully used on rock masses with similar qualities. The $Q$-value can be obtained by using Equation (1).

$$Q = \frac{RQD}{J_n}\frac{J_r}{J_a}\frac{J_w}{SRF} \tag{1}$$

where, $RQD$ is the rock quality designation,
$J_n$ is the joint number,
$J_r$ is the joint roughness,
$J_a$ is the joint alteration,
$J_w$ is the joint water factor, and
$SRF$ is the stress reduction factor.

### 3.3. Stope stability analysis

Bieniawski [14] described ground control as a method to minimise all risks associated with various forms of ground movement and inundation in underground mines within acceptable levels. Therefore, it is imperative that the potentially diverse range of ground characteristics around and within the mine are recognised, and the mine planning and design techniques are well understood before any excavation is made to achieve safe and cost-effective ground control [14].

Numerous studies have discussed various methods used to investigate the stability of stopes; these include empirical, numerical, and statistical method, as well as in-situ test and monitoring methods. The empirical method of analyzing stope stability was proposed by Mathews [15], which entails the use of a stability number (N) to define the bearing capacity of the rock mass to resist failure and hydraulic radius (HR) to denote the geometry of slope face termed stability graph [16]. The numerical approach uses of computer codes such as the FLAC model to assess the stability of open stopes [3].

The statistical method is used to determine the accuracy and probability of stability boundaries [17]. The statistical approach by Mawdesley [18] used logarithm regression analysis to re-examine the stability of the mine. This approach improved the Mathews stability graph by increasing the number of project cases to 500 to quantify the uncertainties of the Mathews design tools [19]. The graph is divided into three segments: the stable area, unstable area and caving zone as shown in Fig. 3. The N-value represents the stability number which denotes the competency of the rock, while the S-value represents the shape factor which is also known as the hydraulic radius (HR), which accounts for the geometry of the surface [19]. In order to improve the reliability of the graph [20] added some transition zones within it, as shown in Fig. 3.

Another important parameter in the evaluation of stope stability in underground excavations is the stope performance (ELOS). It is described as the linear over break or slough of a stope and is an alternative way of expressing the volumetric measurements of the rock over break. It can be calculated using Equation (2).

$$ELOS(m) = \frac{Volume\ overbreak(m^3)}{Surface\ area\ of\ stope\ (m^2)} \tag{2}$$

### 3.4. Ground support and ground reinforcement

The terms ground support and ground reinforcement are often used interchangeably; however, they refer to two different approaches to stabilising rock [22]. Ground support is applied to the excavation

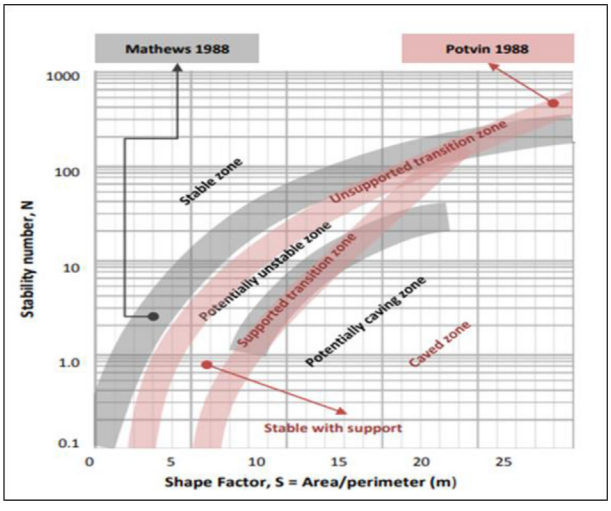


*Fig. 3. Improved Mathews stability graph [21].*

surface, whereas ground reinforcement is installed beyond the excavation surface, deep into the rock. The pillar support system is the most common type of support being used, especially where weak ground conditions are experienced. It is also the only natural type of support; hence its proper design is of great importance. Pillar design in underground mining is a function of two aspects: the pillar strengths; and the stresses acting on the pillars.

According to Stacey [23], "once the pillar strength and pillar stress are known, the factor of safety (FOS) of the pillar can be determined as the ratio of the strength to stress." A FOS of unity is equivalent to a probability of failure of 50%. Stacey [23] argued that "the choice of the FOS value to be used for the design of the pillars and layout depends on the function of the pillars." In most cases, ground support systems complement ground reinforcement elements such as roof bolts, and cable anchors in conjunction with wire mesh and straps.

## 4. Materials and methods

A study of the mine design plan was carried out to determine the extent to which the various stope dimensions had been increased. Survey and geological data were used to analyse and correlate the nature of discontinuities to ground falls.

### *4.1. Rock mass classification*

Reclassification of the mine's rock mass was done in order to account for the changes brought about by water flooding. Reclassification methods, namely physical observations, Rock Tunneling Index, and stability number were used to determine the ground classes and ascertain the rock quality.

#### *4.1.1. Physical observations*

The physical observations entail comparing the properties of the different rock masses found in the stopes. To achieve this, four different stopes with the following conditions were used:

Stope A – not affected by flooding but extended,
Stope B – affected by flooding and extended,
Stope C – affected by flooding but not extended, and
Stope D – not affected by flooding and not extended.

Each of the stopes rock mass was visually assessed, and samples were taken for critical laboratory analyses. Parameters such as the rock strength, joint roughness, joint infill, and the fractures were analyzed. The correlation of jointing to rock falls and to the nature of the surrounding rock mass was noted. This would then predict the likelihood of rock falls in a rock mass with a similar state of jointing as those already observed.

#### *4.1.2. Rock tunneling index*

Joint parameters such as joint alteration, joint number, and joint roughness were used together with the rock quality designation to determine the rock tunneling quality index ($Q$). The ground classes were then assigned based on the range of $Q$-values obtained.

#### *4.1.3. Stability number*

Adopting the same joint parameter values used to calculate $Q$, the modified $Q$ value denoted by $Q'$ was determined. Equation (3), as quoted by Sharp [17] from Barton et al., is used to determine the stability number $N'$.

$$N' = Q'ABC \tag{3}$$

where, $N'$ is the stability number,
$Q'$ is the modified rock tunneling index,
$A$ is the rock stress factor,
$B$ is the joint orientation adjustment factor, and
$C$ is the gravity adjustment factor.

### *4.2. Stope measurements*

The length, width, height, and advance for the different stopes were measured using a distometer. These dimensions were then analysed to see their effect on the stope stability using the hydraulic radius and the stability graph. The stability number $N$, and the shape factor $S$, (hydraulic radius) for each stope were plotted on a stability graph to determine the stability of the stopes.

The advance per blast for each stope was measured on a daily basis for one month. The total of the daily advances divided by the number of days gave the average advance per day. The average daily advance was then extrapolated in order to calculate the expected daily tonnage for each stope. The difference between the expected daily tonnages and the average actual tonnages were used to determine the volume of over break for each of the stopes. Stope performance was also calculated using the volumes of over break, and surface areas of the stopes. ELOS range of values suggested by Mathews [15] were used to determine the stability of the stopes.

### *4.3. Determination of maximum tolerable unsupported length and support method*

The average vertical and horizontal lengths between support holes were measured using

a distometer. The maximum unsupported length was determined using the calculated *Q*-values and excavation support ratio (ESR) values suggested by Mathews [15]. The performance and effectiveness of the installed support elements were analysed regarding to stope heights and ground characteristics to ascertain whether the failures could be attributed to the support elements, the ground conditions, or both. The analysis included studying the support systems that had failed and also that which were susceptible to failure. Investigation of the effectiveness of the available pillars was also done by measuring the pillar dimensions and calculating the pillar strength, stress, and the factor of safety. Fall out heights of falls of ground were measured using a distometer, and these were used to determine the average volume of rock above the roof requiring support. Alternative support elements were then determined based on the support demand for each of the various stopes.

## 5. Results and discussion

This section gives an overview of the research findings, followed by a discussion. The findings are based on the field observations and documented geological, mining, and survey technical reports.

### 5.1. General observations

Discontinuity survey sheets showed that joint structures were dominant and persistent mostly in previously flooded, and extended stopes and major rock falls were common in those stopes. This observation clearly indicated that the formation and extension of fractures during drilling and blasting operations was probably the primary cause of the disintegration, resulting in stope instability. A correlation of the nature of joints to the falls of the ground was done, and the results are shown in Table 1. It was observed that the pervasive carbonate alteration of the host rock (greenstone) occurred during the flooding period, and this made the host rock to be weaker than before; hence it was now fracturing more easily.

A study of the mine plan showed that most of the stopes above 23-level had been extended to almost double their initial size, and expansion of stopes in the levels below 23-level was ongoing. However, this expansion was paying no particular attention to neither the adverse effects imposed by the clearly visible geological discontinuities nor the rock strength deterioration induced by flooding.

### 5.2. Quantification of rock mass quality

The rock masses in the four stopes were studied in order to quantify their quality and subsequently be appropriately classified. The geotechnical parameter conditions of the rock masses in the four stopes were observed, and the results were recorded in Table 2.

#### 5.2.1. Rock quality based on RQD system

The RQD values for the rock masses corresponding to each stope were calculated using Equation (4), and the results are shown in Table 3. The rock classes were assigned based on the standard RQD range of values suggested by Deere [24].

$$RQD = \frac{\sum(Length\ of\ core\ pieces \geq 100\,mm)}{Total\ length\ of\ core\ run} 100 \quad (4)$$

The RQD value for stope A was moderately high with a percentage core recovery of 66%, as shown in Table 3. Following Deere [24] classification, an RQD of 66% falls in the "fair class" suggesting that the rock mass in stope A is partially fractured and fairly competent hence few rock falls are expected in the stope. The fractures present may be mainly due to induced stresses caused by blasting. Percentage core recovery in stope B was 20% which shows that the rock mass was highly fractured; thus, it is very poor and incompetent. Unlike the rock mass in stope A, which is only affected by blast induced stresses, the rock mass in stope B is affected by both the blast induced stresses as well as the pore pressure caused by flooding. Thus, it is valid to have the rock mass in stope B weaker than in stope A.

*Table 1. Correlation between joints and falls of ground.*

| Jointing nature of rock mass | Falls of ground |
|---|---|
| No joints to small minor cracks | Absent |
| Smooth hanging wall (shear plane) without visible joints | Absent |
| Presence of reef sub-parallel shear plane and 1 joint set or 2 joint sets and random joints | Tabular blocks |
| Presence of a narrow shear < 3 m wide or fault zone that is associated with steep and shallow joints without intersecting joints | Blocks |
| Presence of shallow dipping parallel joints with same or opposite dip direction (dip < 45), striking parallel or sub parallel to panel advance direction | Wedge |

*Table 2. Rock mass parameters.*

| PROPERTY | | Stope A | Stope B | Stope C | Stope D |
|---|---|---|---|---|---|
| Strength | Method of assessment | Hand held specimen breaks under more than one blow of a hammer | Cannot be peeled with a knife. Hand held specimen can be broken with one firm blow of a hammer | Hand held specimen breaks under more than one blow of a hammer. | Many hammer blows are required to break an intact specimen |
| | Approx. UCS | 70–150 MPa | ≤ 70 MPa | 70–150 MPa | > 150 MPa |
| Joint filling | | Non-softening sandy particles | Softening clay minerals | Low-friction clay minerals | Clay-free disintegrated rock |
| Joint roughness | | Rough and irregular | Undulating and planar | Slicken-sided planar | Rough and irregular |
| Ground water condition | | Dry excavation | Damp | Damp | Dry excavation |
| Joint spacing | | Very narrow (2–6 mm) | Narrow (6–20 mm) | Very narrow (2–6 mm) | Tight |
| Joint separation | | 60–200 mm | < 60 mm | 60–200 mm | 200–600 mm |
| Persistence of joints | | 60–200 mm | ≥ 200 mm | > 50 mm | 20–40 mm |

*Table 3. RQD results.*

| Stope | RQD value | Rock class |
|---|---|---|
| A | 66 | Fair |
| B | 20 | Very poor |
| C | 52 | Fair |
| D | 88 | Good |

The rock mass in the stope C falls in the "fair" category, thus, implying that it is moderately fractured. An RQD of 52% for the rock mass in stope C suggests that it is slightly more competent than stope B which has a considerably lower RQD. However, the RQD in stope C is lower than in stope A which suggests that the rock mass in stope C is more fractured than that in stope A. The deterioration of rock mass quality in stope C increased due to the weakness induced by the water pressure experienced during the flooding period. If one is to compare the three stopes, it can be deduced that the water pressure enhanced the deterioration of the rock mass quality than what is caused by blast induced stresses. Nonetheless, the combined effect of the two is evidently catastrophic. Stope D has the highest value of RQD of 88%, which shows that the rock mass in this stope has the least frequency of fractures as compared to the other three stopes. The fewer fractures in rock mass may be attributed to mild effects caused by mining operations which took place in this region prior the flooding era.

### *5.2.2. Rock quality based on the Q-system*

The Rock Quality Index ($Q$) depends on three parameters: the degree of jointing, joint friction, and active stress. The three parameters were calculated for each of the four stopes, and the results are shown in Table 4. These parameters were then used to determine the $Q$-values, which are also shown in Table 4.

The extension of stope A caused some substantial stress redistribution in the rock mass such that the stress magnitude became slightly more significant than the rock strength, hence the moderate $Q$-value of 6.6. The low $Q$-value obtained in stope B (approx. 0.17) is mainly due to the lower active stress which, in turn, was caused by a lower joint water reduction factor $J_w$. In addition, the softening clay joint filling

*Table 4. Rock quality index parameters.*

| Stope | Degree of jointing | Joint friction | Active stress | $Q$-values |
|---|---|---|---|---|
| A | 11.00 | 1.500 | 0.4000 | 6.6 |
| B | 6.67 | 0.375 | 0.0667 | 0.17 |
| C | 17.33 | 0.375 | 0.1320 | 0.86 |
| D | 14.67 | 1.500 | 1.000 | 22 |

in the undulating and planar joints observed on this rock mass implies some low joint friction which cause the rock mass to be of poor quality. To this point, it is logical to have stope B being the most unstable of the four stopes in consideration.

In general, stope stability increases if the stope is cut in a rock mass with a high degree of jointing; thus stope C is expected to be relatively stable. However, by having a low active stress value due to the stope's high SRF and the low $J_w$, the stability of the stope is significantly reduced. A low $Q$-value of 0.86 for stope C indicates that a combination of low active stress and low joint friction, due to clayey minerals found in the slicken-sided planar joints, makes stope C highly unstable despite the high degree of jointing. A substantially high $Q$-value of 22 was obtained on the rock mass in stope D. The absence of water, favourable stress conditions in the region, and the presence of clay-free disintegrating rock joint infill in rough and irregular joints (high joint friction) aided in having the rock mass in stope D to be of high quality. A stope cut in a rock mass of high quality is expected to be stable; thus stope D should be highly stable.

#### 5.2.3. Evaluation of the stability number ($N'$)

The stability number was also used to assess the stability of the stopes. The assessment was dependent on the modified $Q$-value ($Q'$), the rock stress factor (A), the joint orientation adjustment factor (B), and the gravity adjustment factor (C). The $Q'$-values were calculated using Equation (5), and the results are presented in Table 5. Parameter values for the stability factors A, B, and C, shown in Table 5, were adopted to calculate of $N'$ using Equation (3).

$$Q' = \frac{RQD}{Jn}\frac{Jr}{Ja} \tag{5}$$

According to Hoek [25] "failure occurs along critical joints which form a shallow angle with the free face." Therefore, basing the stability of stope A on the $B$-value of 0.2 alone means that the stope was likely to fail. However, the rock mass in stope A had a high $A$-value of 0.7, which caused the stope's stability number $N'$ to be fairly high (approx. 16). Stope B's stability number of 2, shows that the stope is the most unstable. Ideally, it should have been the most stable since the critical joints in the stope form the widest angles ($\approx$600). However, the low $A$ and $Q'$ values greatly decreased its stability number, causing it to be the most unstable stope.

Although the stability number for stope C is considerably low (approx. 5) due to the shallow angles between the critical joints in the stope, a fairly high rock stress factor of 0.5 makes the stope to be more stable when compared to stope B. Stope D has the highest stability number of approx. 25, compared to the other stopes thus it is the most stable. This is mainly attributed to the stope's high $Q'$-value of 22 and a high $A$-value of 0.8. These high $Q'$ and $A$ values alter the adverse effect of shallow angles' between the stope's critical joints. It is worth noting that the value of the gravity adjustment factor ($C$) was the same in all the stopes, hence its effect in comparing the stability of the stopes was insignificant.

### 5.3. Determination of the hydraulic radius

The hydraulic radii for the stopes, shown in Table 6, were calculated using Equation (6). Stopes A and B have higher hydraulic radii compared to stopes C and D. This is mainly attributed to the fact that stopes A and B have been extended, implying that they are larger than stopes B and C. Generally, the higher the hydraulic radius, the higher the susceptibility of stope to instability, thus stope instability is expected to decreases from stopes A to D. The trend would be such that stope A would be the most unstable, whereas stope D would be the most stable.

$$\textit{Hydralic radius} = \frac{wh}{2(w+h)} \tag{6}$$

where, $w$ and $h$ are the width and height of stope respectively.

### 5.4. Determination of stope stability using the stability graph

The calculated values of the stability number ($N'$) and shape factor ($S$, hydraulic radius) for the stopes

*Table 5. Modified Q-values.*

| Stope | Joint orientation | $B$-value | $A$-value | $C$-value | $Q'$-values | $N'$ |
|---|---|---|---|---|---|---|
| A | 20 | 0.2 | 0.7 | 7 | 16.5 | 16.17 |
| B | 60 | 0.6 | 0.2 | 7 | 2.5 | 2.10 |
| C | 30 | 0.3 | 0.5 | 7 | 6.5 | 5.04 |
| D | 20 | 0.2 | 0.8 | 7 | 22 | 24.64 |

*Table 6. Stope hydraulic radius.*

| Stope | Height (m) | Width (m) | Area ($m^2$) | Perimeter (m) | Hydraulic radius (m) |
|---|---|---|---|---|---|
| A | 41 | 38 | 1558 | 158 | 9.86 |
| B | 35 | 30 | 1050 | 130 | 8.08 |
| C | 24 | 15 | 360 | 78 | 4.62 |
| D | 18 | 11 | 198 | 58 | 3.41 |

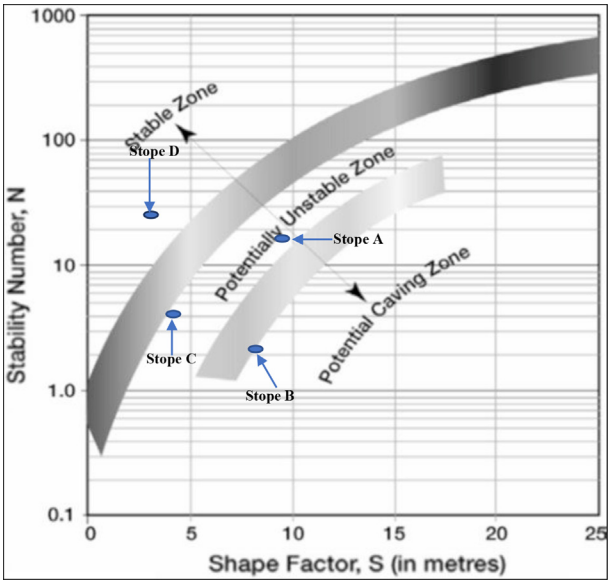


*Fig. 4. Determination of stope stability on the stability graph.*

were used to ascertain the stability of the stopes using the stability graph in Fig. 4. The effect of stope extension, flooding, and a combination of the two was clearly brought out. Stope A and stope C both fell in the potentially unstable zone. Although stope A was not affected by water, its high hydraulic radius shows that it has been significantly extended, and this caused some alterations in the stope's stress distribution, thereby making it potentially unstable. On the other end, the low hydraulic radius of stope C indicates that the stope has not been extended; hence the stope has been made potentially unstable solely due to the increase in pore pressure caused by flooding. It can thus be deduced that both flooding and stope extension induce some instability in the rock mass.

Stope B lies in the potentially caving zone, and the stope is highly unstable. Since the stope was extended after the flooding era, it can be concluded that the combined effect of pore pressure and mining induced stresses greatly affects the stability of the stope. Stope D falls in the stable zone because it has the highest stability number and the lowest hydraulic radius. Since the stope has neither been extended nor affected by flooding, the mining induced stress remained evenly distributed hence making it highly stable.

### *5.5. Analysis of stope performance (ELOS)*

ELOS values for the stopes were calculated using Equation (2). The data for daily advances, expected tonnage, and over-break volumes, which is required for the determination of ELOS, values is presented in Table 7 below.

Mathews [15] came up with a standard system that puts the ELOS values into ranges corresponding to the likely type of stope. The ELOS for the stope A (0.83) falls in of 0.75–2 m where limited failure is expected from the unsupported stope. This is due to the considerably low volume of over break since the rock mass in this stope had not been affected by flooding. Hence, the stope was less susceptible to blast damage. Severe sloughing and huge failure volumes should be expected on stope B if the stope walls are left unsupported. The ELOS value of 2.52 is mainly due to the high over break experienced as a result of the high fractured rock in the stope, and wall collapse is highly possible. The high deterioration of the rock mass in stope B can be attributed to a combination of blast induced damage and the weakening effect of water caused by flooding.

The high volume of over break experienced over a small stope face puts stope C in the unstable zone. The quality of the rock mass in this stope was considerably deteriorated due to flooding. Thus, minor to moderate sloughing of the stope walls should be anticipated. An ELOS value of 0.49 for stope D is classified under the stable zone. The ELOS value was the lowest because the volume of over break was small since the rock mass in this region was competent. Rock mass competence in this stope is possible since the stope had not been affected by both flooding and blasting disturbances. The stope walls can therefore be expected to be self-supporting.

### *5.6. Correlation between ELOS and hydraulic radius*

Figure 5 shows a plot of the hydraulic radius against the ELOS used to determine the factor that influences the quality of the rock mass to a greater extent. Stopes A and B were expected to have the

*Table 7. Stope performance (ELOS) data.*

| Stope | Expected volume ($m^3$) | Actual volume ($m^3$) | Over-break volume ($m^3$) | Area ($m^2$) | ELOS (m) |
|---|---|---|---|---|---|
| A | 2555.12 | 3853.12 | 1298 | 1558 | 0.83 |
| B | 1837.5 | 4480.5 | 2643 | 1050 | 2.52 |
| C | 622.8 | 1202.8 | 580 | 360 | 1.61 |
| D | 306.9 | 402.9 | 96 | 198 | 0.48 |

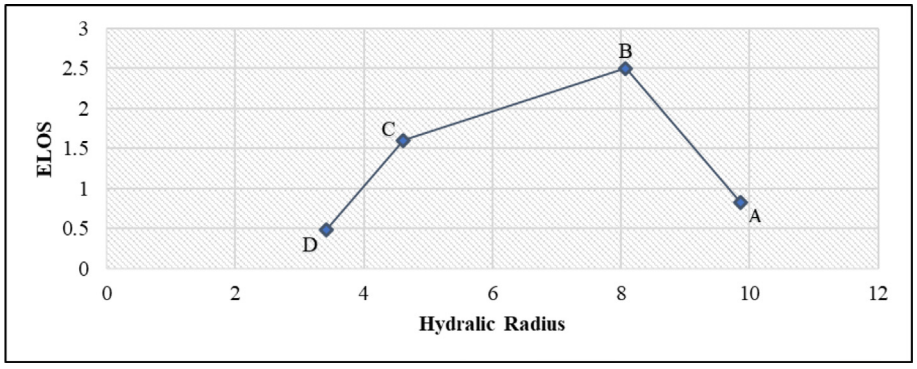


*Fig. 5. ELOS versus hydraulic radius.*

most over-break since they had the largest values of the hydraulic radius. However, it can be observed that the over break in stope C was greater than that in stope A despite it having a small hydraulic radius. Therefore, it can be deduced that although stope extension plays a part in the over-break experienced in different stopes, it is not the main cause of the overall stope instability. The relationship suggests that over-break is highest in the stopes affected by flooding, that is in stopes B and C. This result confirms the supposition that over-break is largely controlled by pore pressure than it is by blast induced stresses.

### *5.7. Determination of the maximum tolerable unsupported length*

After ascertaining the ground conditions, there was need to determine the maximum length that could be left unsupported for each stope. Stillborg [22] came up with a formula to calculate the maximum tolerable unsupported length, Equation (7).

$$\textit{Maximum unsuppported length} = 2\,ESR\,Q^{0.4} \qquad (7)$$

where, *ESR* is the excavation support ratio which is empirically deduced and *Q* is the *Q*-value deduced from the *Q*-system.

Thus, in this case an ESR value of 1.6, assigned on permanent mine openings as proposed by Mathews [15] was adopted in the calculation of the maximum unsupported length for the four stopes. The calculated values were then compared with the actual measured lengths of the unsupported spans in each stope and the data is tabulated in Table 8 below.

From Table 8, it can be deduced that stopes A and D can be extended to approx. 6.8 and 11 m, respectively, without requiring any support installation. Although, the standard unsupported span of 3.9 m being used at the mine is lower than the maximum tolerable unsupported lengths for stopes A and D, it is greater than that which can be tolerated in stopes B and C. Therefore, if stopes B and C are left unsupported ground failure is likely to occur. This can be taken as a clear indication that the ground quality in stopes B and C has significantly deteriorated. Although, the ground in stopes B and C could be extended with no adverse consequences prior to flooding, it now requires some additional support at spans less than the standard mining span of 3.9 m.

*Table 8. Maximum tolerable unsupported length.*

| Stope | Actual unsupported span (m) | Maximum tolerable unsupported length (m) |
|---|---|---|
| A | 3.9 | 6.8 |
| B | 3.9 | 1.6 |
| C | 3.9 | 3.0 |
| D | 3.9 | 11.0 |

### *5.8. Support design*

The current support system being implemented at the mine comprises mat packs, natural in-situ pillars, and timber props. The study showed that the stability of timber props decreased with increasing the height and length of the stopes. Timber props in stope D were highly stable, whereas those in stopes A and B buckled at various panel lengths. The stability of mat packs also decreased with increasing stope height. Daehnke [26] mentioned that "it is commonly assumed that timber packs with a height-to-width ratio exceeding 2:1 are unstable, particularly during dynamic closure." Hence, the use of mat packs in stope A and B was no longer effective as the height-to-width ratio of 2:1 had been exceeded. Falls of ground were now prevalent in these stopes, thus showing that the mat pack support systems had been rendered ineffective.

In-situ pillars of 4 × 4 m in dimension are left out as support in most of the stopes at the mine. In the

very bad ground, the pillar size is increased to 5 × 5 m. Pillar spalling became the major problem with these natural in-situ pillars mainly due to excessive overburden stresses. Pillar overloading was due to the significantly increased stope dimensions while maintaining the same pillar dimensions. As a result, the recommended factor of safety of 1.6 on hard rock pillars was lowered beyond this point such that the pillars were now ineffective. Table 9 shows the average safety factors for the four stopes. The pillar strengths have been calculated with the design rock mass strength (D.R.M.S) assumed to be 37.5% of the UCS. The pillar strength is calculated using Equation (8).

$$Pillar\ strength = D.R.M.S\ W^{0.5}/H^{0.75} \quad (8)$$

where, W is the pillar width, and

H is the pillar height.

To determine the support demand, the average thickness of rock requiring support should be determined. The average thickness was estimated by averaging the fall-out heights that had been recorded in each of the stopes, and these are shown in Table 10. The support demand per square meter was calculated using Equation (9).

$$Support\ Demand/m^2 = \rho gh \quad (9)$$

where, $\rho$ is the density of the rock (taken to be 2700 kg/m$^3$),

$g$ is the acceleration due to gravity, and

$h$ is the rock block thickness (average fall-out height).

Using the calculated rock support demand for the various stopes and the maximum load carrying capacities of different support elements on the market, the appropriate support elements to be used in each stope were ascribed, as shown in Table 11 below. The recommended support systems are not only based on the support demand but also the maximum tolerable area and the factor of safety for the varying ground conditions.

## 6. Conclusion and recommendations

The mine under review involved mining infrastructure affected by flooding, which has caused the rock mass quality to significantly deteriorate. Mining has been progressing well during the post-flooding era up until 21-level, where it is now very evident that the stopes below this level are now highly unstable and the support method is now incompatible with the new ground conditions. The research has been prompted to investigate the causes of stope instabilities at Golden Valley Mine and consequently, provide an alternative compatible support system.

It can be concluded that the pervasive carbonate alteration that occurred in the host rock during the flooding period has clearly weakened the rock mass. The development of numerous fractures upon a single blast is confirmation that the rock mass strength has substantially deteriorated. These fractures have a great adverse effect on the quality of the rock mass, which ultimately causes stope instabilities. In addition to blast induced fractures, high pore pressure in the moderately altered joint walls in post flooded excavations has caused washing out of most joint fillings, thereby inducing ground failure along these discontinuities. Falls of ground have now been so prevalent in the previously flooded stopes as was noticed in stopes B and C, in which the maximum tolerable unsupported lengths have been significantly reduced.

*Table 9. Factor of safety for the pillars in the various stopes.*

| Stopes | Average virgin stress (MPa) | Pillar dimensions | | | Effective pillar width (m) | Areal extraction (in panel) (%) | Pillar strength (MPa) | Pillar stress (MPa) | Safety factor |
|---|---|---|---|---|---|---|---|---|---|
| | | Pillar length (m) | Pillar width (m) | Height (m) | | | | | |
| A | 4.8 | 4 | 4 | 2.5 | 4 | 86.8 | 41.495 | 36.4 | 1.14 |
| B | 5.1 | 5 | 5 | 2.5 | 5 | 92.5 | 29.523 | 68.0 | 0.43 |
| C | 5.1 | 5 | 5 | 2.5 | 5 | 82.5 | 46.393 | 29.1 | 1.59 |
| D | 4.8 | 4 | 4 | 2.5 | 4 | 80.8 | 56.585 | 25.0 | 2.26 |

*Table 10. Average fall-out height and support demand.*

| Stope | Fall-out heights (m) | | | | | Cumulative fall-out height (m) | Average fall-out height (m) | Support demand/m$^2$ (kN) |
|---|---|---|---|---|---|---|---|---|
| | 1 | 2 | 3 | 4 | 5 | | | |
| A | 1.56 | 0.97 | 1.65 | 1.11 | 1.34 | 6.63 | 1.33 | 35 |
| B | 3.20 | 3.41 | 3.52 | 2.90 | 3.95 | 17.0 | 3.40 | 90 |
| C | 2.88 | 3.20 | 2.90 | 2.78 | 2.43 | 14.2 | 2.84 | 75 |
| D | 0.41 | 0.32 | 0.43 | 0.47 | 0.36 | 1.99 | 0.40 | 11 |

*Table 11. Recommended support systems.*

| Support element specifications | | Stope support pattern | |
|---|---|---|---|
| Support element | Load bearing capacity | Stope | Recommended support elements |
| Timber props | 50 kN | **A** | • Timber props spaced at 4 m apart<br>• 4 × 6 m in-situ pillars |
| Mat packs | 80 kN | **B** | • 20 mm anchored rock studs spaced 2 m apart or 16 mm cone bolts spaced at 1 m apart<br>• 6 × 8 m in-situ pillars |
| Roof bolts (Shepherd's Crook cone bolts) | 16 mm–100 kN | **C** | • 16 mm rock studs spaced at 2 m apart<br>• 6 × 8 m in-situ pillars |
| Anchored rock stud | 20 mm–200 kN<br>16 mm–150 kN<br>13.5 mm–100 kN | **D** | • Timber props spaced at 4 m apart<br>• 4 × 4 m pillars |

It was also clearly seen that stope stability is adversely affected by increased stope dimensions. This effect can be attributed to the redistribution of stresses to the rock mass surrounding the stopes such that the in-panel pillars will be highly stressed, thereby triggering stress induced ground failures. The stress induced failure would manifest as spalling or slabbing on the pillars, and in some instances, it manifested in the form of small rock bursts. In addition, to release this stress, rock masses tend to fracture with ease, leading to stope over-breaks. As a result, smaller excavations (those that have not been extended) such as stopes C and D are likely to be more stable. It can be deducted that stability in stopes C and D has been caused by the low hydraulic radii, contrary to the high hydraulic radii in stopes A and B. The deduction is premised on the fact that the higher the hydraulic radius, the higher the susceptibility of stope to instability. It was observed that over-break was highest in stopes which were affected by flooding, that is in stopes B and C. The high over-break shows that the water invasion in mining excavations has a greater influence on stope stability.

The support system in any excavation depends on the quality of the rock mass and the stopes support demand. Therefore, incompetent rock masses such as that in stope B require some comprehensive support systems involving support elements that are closely spaced in order to counter major rock falls. The varying ground conditions entail different maximum tolerable unsupported lengths and support systems. Thus, the implementation of a support system should never be a one size fits all without considering the rock characteristics, or else the support system is rendered inefficient.

Rectangular pillars should be used instead of square pillars since they are highly capable of abating ground failure imposed by high horizontal stresses being incurred at the mine. The mine should implement 6 × 8 m pillars which have proved to have an acceptable factor of safety against failure. However, in areas where it is observed that the ground is excessively weak, the dimensions should be changed to suit such conditions. In addition, a ground monitoring program should be implemented in order to monitor the performance of the ground support systems. For this to be effective, there is a need to consider installing support elements coupled with electronic sensors which give early warning signs in real time. This will allow the timeous evacuation of personnel and equipment from the danger zones.

## Conflicts of interest

We declare that the information disclosed is correct and no conflict of interest is known to us.

## Ethical statement

The research was conducted according to ethical standards.

## Funding body

This research received no external funding.

## Acknowledgements

The authors would like to thank Golden Valley Mine for providing access to the data that was used in this paper. Permission to access unpublished, usually confidential information, is greatly appreciated.

## References


[1] Villaescusa E. Quantifying open stope performance. Proceedings of Mass Min 2004 Aug:96–104.

[2] Kolapo P, Munemo P. Investigating the correlations between point load strength index, uniaxial compressive strength and Brazilian tensile strength of sandstones. A case study of QwaQwa sandstone deposit. Int J Min Miner Eng 2021;12(1): 67–83.

[3] Ma Saiang D, Nordlund E. Numerical analyses of the effects of rock mass property variability on open stope stability. In: The 45th US rock mechanics/geomechanics symposium. OnePetro; 2011 Jun 26.

[4] Swart AH, Handley MF. The design of stable stope spans for shallow mining operations. J South Afr Inst Min Metall 2005 Apr 1;105(4):275–86.

[5] Google Maps. Golden Valley Mine. [Internet] [cited 2021 Jul 21]. 2021. Available from: https://google.com/maps/dir/Kwekwe/Golden+Valley+Mine.

[6] Stacey TR, Page CH. Practical handbook for underground rock mechanics. 1986.

[7] Kolapo P. Investigating the effects of mechanical properties of rocks on specific energy and penetration rate of borehole drilling. Geotech Geol Eng 2021 Feb;39(2):1715–26.

[8] Brahimaj F, Dambov R. Impact of some physical-mechanical and structural characteristics of slope stability. In: Proceedings of the VII international geomechanics conference, Varna, Bulgaria; 2018.

[9] Stacey TR. Best practice rock engineering handbook for "other" mines. SRK Consulting. Project Number: OTH. 2001 Dec:602.

[10] Lauffer H. Mountain classification for tunnel construction. Geol Construct 1958;24(1):46–51.

[11] Gundewar CS. Application of rock mechanics in surface and underground mining. Indian Bureau of Mines 2014:165.

[12] Pacher F, Rabcewicz L, Gosler J. On the side of the rock classification in gallery and tunnel construction. 1974.

[13] NGI. Using the Q-system: rock mass classification and support design. Oslo: Nowergian Geotechnical Institute; 2015.

[14] Bieniawski ZT. Engineering rock mass classifications: a complete manual for engineers and geologists in mining, civil, and petroleum engineeringvol. 24. John Wiley & Sons; 1989 Aug.

[15] Mathews K, Hoek E, Wyllie D, Stewart S. Prediction of stable excavations for mining at depth below 1000 meters in hard rock. Ottawa (CA): Department of Energy, Mines and Resources; 1981.

[16] Saadaari F, Mireku-Gyimah D, Olaleye B. Development of a stope stability prediction model using ensemble learning techniques - a case study. Ghana Min J 2020 Dec 31;20(2):18–26.

[17] Sharp JE. Applicability of the Mathews stability method to open stope stability assesment at Olympic Dam Mine. MSc [thesis]. Christchurch: University of Canterbury; 2011.

[18] Mawdesley C. Using logistic regression to investigate and improve an empirical design method. Int J Rock Mech Min Sci 2004 May 1;41:756–61.

[19] Zhang L, Hu JH, Wang XL, Zhao L. Optimization of stope structural parameters based on Mathews stability graph probability model. Adv Civ Eng 2018 Jan 1:1–8.

[20] Potvin Y. Empirical open stope design in Canada. PhD [dissertation]. Vancouver: University of British Columbia; 1988.

[21] Jang HD. Unplanned dilution and ore-loss optimisation in underground mines via cooperative neuro-fuzzy network. PhD [dissertation]. Perth: Curtin University; 2014.

[22] Stillborg EB. Professional users handbook for rock bolting. 2nd ed. Zurich: TransTech Publishers; 1994.

[23] Stacey TR, Swart AH. Practical rock engineering practice for shallow and opencast mines. Safety in Mines Research Advisory Committee; 2001.

[24] Deere DU, Hendron AJ, Patton FD, Cording EJ. Design of surface and near surface construction in rock. In: The 8th US symposium on rock mechanics (USRMS). OnePetro; 1966 Sep 15.

[25] Hoek E, Kaiser PK, Bawden WF. Support of underground excavations in hard rock. CRC Press; 2000.

[26] Daehnke A, Van Zyl M, Roberts MK. Review and application of stope support design criteria. J South Afr Inst Min Metall 2001 May 1;101(3):135–64.